



Integrated 1D-2D Resistivity Inversion for Mapping Seawater Intrusion in a Coastal Aquifer: Kenjeran-Surabaya, Indonesia Case Study

Himatul Farichah¹, Bagas Aryaseta^{1*}, Aulia Dewi Fatikasari¹, Dini Oktavia¹

¹Faculty of Engineering and Science, Universitas Pembangunan Nasional Veteran Jawa Timur, Jl. Raya Rungkut Madya, Surabaya 60294, East Java, Indonesia

* bagas.aryaseta.ts@upnjatim.ac.id

Abstract. This study investigates the extent of intrusion in the Kenjeran coastal aquifer, Surabaya, Indonesia, through an integrated geophysical approach. Four one-dimensional Vertical Electrical Sounding (VES) surveys and two two-dimensional Electrical Resistivity Tomography (ERT) transects were conducted using Schlumberger and Wenner-Schlumberger configurations to obtain both depth-specific and laterally continuous resistivity data. The 1D VES results detected low-resistivity layers ($<1.0 \Omega \cdot m$) at depths exceeding 58–66 m, indicating deep saline groundwater. The 2D ERT sections identified wedge-shaped low-resistivity anomalies ($0.1–0.8 \Omega \cdot m$) at depths of 7.5 m to 48 m, indicating active intrusion progressing inland. Intrusion is more severe in the northern sector, with vertical penetration up to 48 m and horizontal encroachment beyond 200 m from the shoreline. The integration of 1D and 2D resistivity imaging proved effective in delineating saline–freshwater interfaces, enabling targeted mitigation measures and informed groundwater management to safeguard Kenjeran’s aquifer from further degradation.

Keywords: Coastal aquifer, electrical resistivity tomography, saline groundwater, seawater intrusion, vertical electrical sounding

(Received 2025-08-16, Revised 2026-01-21, Accepted 2026-01-23, Available Online by 2026-01-31)

1. Introduction

Coastal aquifers are critical sources of freshwater for domestic, agricultural, and industrial purposes, especially in densely populated urban regions. However, these aquifers are increasingly threatened by seawater intrusion—a process where saline water infiltrates freshwater zones, thereby degrading groundwater quality and posing serious risks to human health, agricultural productivity, and coastal ecosystems [1], [2], [3]. This phenomenon typically results from a disruption in the natural hydraulic balance between freshwater and saltwater, often caused by excessive groundwater extraction, rapid urbanization, and sea-level rise associated with climate change [4], [5], [6].

In Indonesia, the impacts of seawater intrusion have become increasingly evident in several urban

coastal zones. Rapid population growth, industrial expansion, and uncontrolled groundwater abstraction have collectively contributed to the depletion of groundwater levels and the salinization of freshwater resources [7], [8], [9]. Surabaya—the second-largest city in Indonesia—illustrates these challenges. The eastern coastal area of Surabaya, including the Kenjeran district, has undergone rapid land-use transformation, particularly with the development of residential and industrial areas. These changes have led to increased reliance on groundwater and the discharge of industrial and domestic waste into the subsurface, both of which contribute to the deterioration of groundwater quality across the city's coastal fringe [10]. Previous studies have also reported the presence of seawater intrusion in other parts of Surabaya's coastline [11], [12]. Kenjeran, located on the northern coast of Surabaya and bordering the Madura Strait, is one of the areas exhibiting early signs of seawater intrusion, including elevated salinity levels in shallow wells [13], [14]. A recent geoelectrical investigation confirmed the potential for saline water encroachment in this district [15]. The combination of geological settings and anthropogenic pressures makes Kenjeran a suitable case study for investigating seawater intrusion dynamics in a tropical coastal environment.

A comprehensive understanding of the spatial extent and subsurface distribution of seawater intrusion is critical for developing effective groundwater protection strategies and long-term water resource management. Geophysical methods, particularly ERT, offer a robust, non-invasive, and cost-effective means of delineating subsurface features and mapping saline–freshwater interfaces [16]. ERT measures variations in electrical resistivity, which can be interpreted to distinguish different lithologies and fluid saturations. Since saline water exhibits significantly lower resistivity than freshwater, this method is particularly well-suited for mapping the progression of seawater intrusion. ERT has been successfully employed in various coastal aquifer studies, including time-lapse monitoring in Mediterranean regions using cross-hole ERT (CHERT) [17], large offset ERT along the California coast for fresh/salt interface mapping [18], and high-resolution imaging in urbanized coastal plains to delineate saltwater wedges [19]. Furthermore, integrating 1D VES and 2D ERT datasets provides a more comprehensive and reliable characterization of aquifer conditions. The combination of 1D VES, which delivers detailed vertical resistivity variations, with 2D ERT data, which maps lateral resistivity distribution, enables a more accurate delineation of saltwater-contaminated aquifer zones in coastal areas [20], [21], [22].

Despite the established application of these methods in various coastal settings, seawater intrusion studies using resistivity-based approaches have never been conducted in the Kenjeran coastal area, which is known to be highly vulnerable to saline intrusion. Previous investigations were limited to the Sutorejo area—approximately 5 km from Kenjeran—and employed induced polarization and 2D ERT methods [13], [23]. Consequently, the absence of resistivity-based seawater intrusion assessments in Kenjeran represents a significant research gap that this study aims to address. This study aims to investigate the presence and spatial distribution of seawater intrusion in the coastal aquifer of Kenjeran, Surabaya, integrating 1D VES and 2D ERT surveys. The specific objectives are to: (1) conduct 1D VES measurements to define the vertical resistivity structure and estimate the depth of saline groundwater zones; (2) perform 2D ERT surveys to delineate the lateral and spatial distribution of seawater intrusion; and (3) validate and contextualize the Kenjeran results by comparing them with similar resistivity-based studies conducted in nearby coastal locations. By applying integrated geophysical methods and resistivity modeling, this research contributes to a deeper understanding of seawater intrusion processes and offers critical insights for the protection and sustainable development of groundwater in urban coastal environments.

2. Methods

2.1. Study Area

The geoelectrical survey was conducted in the coastal zone of Kenjeran, specifically within the Kedung Cowek neighborhood, Bulak Subdistrict, Surabaya City, East Java Province, Indonesia. The study area lies near the Madura Strait, positioned roughly 200 m from the shoreline and around 300 m from a

densely populated residential areas. The terrain is generally flat with a low elevation of 1–3 m above sea level and is underlain by unconsolidated Quaternary alluvial sediments. These geological and hydrogeological characteristics make the local aquifer system particularly vulnerable to seawater intrusion. The surrounding area is predominantly used for rice cultivation, highlighting the socioeconomic importance of freshwater resources and the region's sensitivity to groundwater salinization.

2.2. Survey Layout

As illustrated in Figure 1, the survey layout included four 1D VES stations (G1–G4) and two 2D ERT profiles (Line 1 and Line 2), each with clearly defined end points (Line 1' and Line 2'). The two ERT lines, each about 230 m long, were positioned to cross the expected pathways of seawater intrusion and to capture the transition between saline and freshwater zones. The arrangement of the profiles and sounding points was planned to ensure adequate spatial coverage of the subsurface, allowing a more integrated interpretation of the aquifer system and the extent of intrusion.

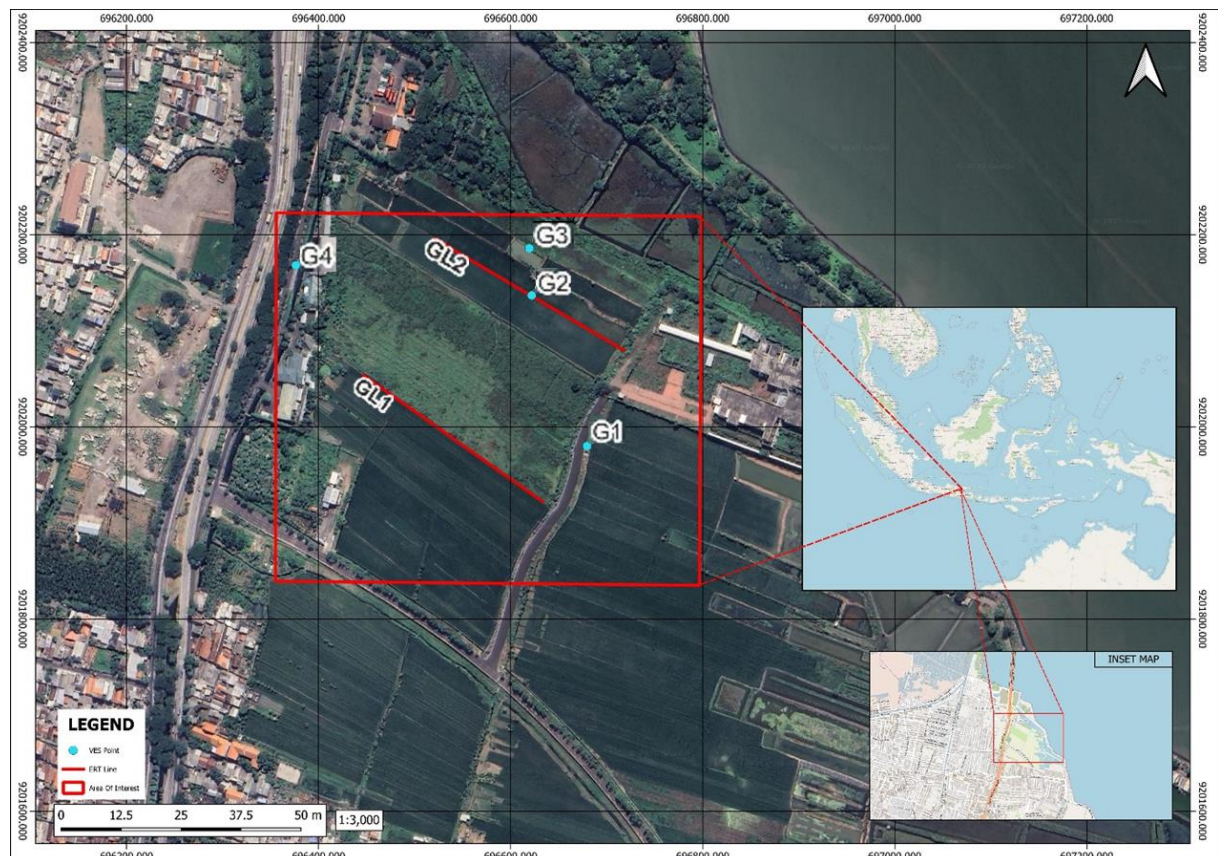


Figure 1. Location of 1D VES and 2D ERT Survey in Kenjeran, Surabaya

2.3. 1D - Vertical Electrical Sounding (Schlumberger Configuration)

Four 1D VES soundings (G1–G4) were conducted using the Schlumberger array. The current electrode spacing ($AB/2$) was expanded progressively from 1.5 m to a maximum of 100 m, while potential electrode spacing ($MN/2$) was adjusted at 0.5, 1, 5, 10, and 25 m depending on signal strength and depth of investigation. The field measurements consisted of electrode spacings ($AB/2$ and $MN/2$), injected current (I), and measured potential difference (V). Apparent resistivity was computed using the Schlumberger geometric factor (K).

To maintain data quality, stainless-steel electrodes were deployed, and contact resistance was controlled to remain below approximately 800 Ω through soil wetting and repeated grounding when

necessary. Each datum was stacked 3–5 times to improve the signal-to-noise ratio, and reciprocity checks were performed at selected electrode spacings to evaluate acquisition consistency. Measurements exhibiting anomalously low apparent resistivity ($<0.01 \Omega \cdot \text{m}$), excessively high contact resistance, or standard deviations exceeding 5% were discarded during quality control. The filtered datasets were processed and inverted using the IPI2Win software based on a layered-earth forward modeling approach. The inversion produced 1D resistivity models together with apparent resistivity curves and pseudosections for each sounding. These results provide quantitative constraints on lithological layering, aquifer depth, and the potential occurrence of seawater-intruded zones [24], [25].

2.4. 2D – Electrical Resistivity Tomography (Wenner-Schlumberger Configuration)

Two 2D ERT profiles were acquired to characterize the lateral and vertical distribution of subsurface resistivity and to delineate the freshwater–saltwater interface. Data were collected using the Wenner-Schlumberger configuration, selected for its balanced sensitivity to both horizontal and vertical resistivity gradients, which is advantageous for resolving salinity transitions and lithological heterogeneity in coastal aquifers [26], [27]. Each profile (GL1 and GL2) was approximately 230 m in length and consisted of 24 stainless-steel electrodes spaced at 10 m intervals.

Contact resistance was monitored throughout the survey and maintained within acceptable limits (typically $<900 \Omega$) through soil wetting and repeated electrode grounding when necessary. Each measurement was stacked 3–6 times to improve the signal-to-noise ratio, and reciprocal readings were acquired at selected electrode combinations to evaluate data reliability. Noisy readings, negative apparent resistivity values, and measurements with high standard deviations were removed during quality control.

Apparent resistivity values (ρ_a) were inverted for each profile using Res2DInv, which applies a smoothness-constrained least-squares algorithm to obtain true resistivity distributions. A model was accepted when the inversion error reached a sufficiently low RMS misfit. The inversion produced resistivity cross-sections and pseudosections for each line. The resulting resistivity cross-sections display the distribution of true resistivity values at depth, with color gradations indicating variations in lithology and saturation. These models provide essential constraints for identifying subsurface layering, aquifer characteristics, and zones potentially affected by seawater intrusion.

3. Results and Discussion

3.1. 1D Resistivity Profiles

Table 1. Summary of 1D Resistivity Measurements from VES Points G1–G4

G1		G2		G3		G4	
Depth (m)	Resistivity (Ωm)	Depth (m)	Resistivity (Ωm)	Depth (m)	Resistivity (Ωm)	Depth (m)	Resistivity (Ωm)
0 – 1.3	447	0 – 2.84	3.82	0 – 0.335	9.43	0 – 0.172	65.2
1.3 – 4.36	61.5	2.84 – 64.9	1.07	0.335 – 1.33	3	0.172 – 0.902	233
4.36 – 14.9	0.503	>64.9	0.118	1.33 – 66.1	1.09	0.902 – 2.74	8.21
14.9 – 62.6	2.21			>66.1	0.115	2.74 – 58.3	1.72
>62.6	0.104					>58.3	0.12

The 1D VES interpretations for points G1–G4 (Table 1) reveal distinct vertical variations in resistivity that are consistent across the study area. These variations were interpreted by comparing the measured values with commonly accepted resistivity thresholds for lithology and groundwater salinity conditions [16]. A clear pattern emerges at all four points: high resistivity in the shallow unsaturated zone, intermediate values in the brackish transition zone, and very low resistivity at depth attributable to saline intrusion.

Low-resistivity layers ($<0.5 \Omega \cdot \text{m}$) were identified at depths $>58\text{--}66 \text{ m}$ at all VES locations. While the reviewer notes that such values may also indicate marine clay or organic-rich sediments, this interpretation is less consistent with the known subsurface geology of eastern Surabaya. Regional stratigraphic records and engineering borehole data from the Surabaya coastal plain indicate that the Quaternary deposits in Kenjeran are dominated by sandy to silty alluvium with minor clay lenses, lacking thick organic layers or expansive marine clay formations that would typically produce persistent low-resistivity responses. Moreover, the extremely low resistivity values recorded ($0.104\text{--}0.12 \Omega \cdot \text{m}$) fall well below the resistivity range of typical clay-rich formations (generally $1\text{--}10 \Omega \cdot \text{m}$), but are fully consistent with saline-saturated groundwater.

At G1, a distinct low-resistivity zone ($0.503 \Omega \cdot \text{m}$ at $4.36\text{--}14.9 \text{ m}$ and $0.104 \Omega \cdot \text{m}$ below 62.6 m) indicates strong saline influence, with an intermediate brackish interval ($2.21 \Omega \cdot \text{m}$ at $14.9\text{--}62.6 \text{ m}$). G2 exhibits a similar pattern, with saline groundwater inferred below 64.9 m ($0.118 \Omega \cdot \text{m}$) and a brackish zone extending upward to 2.84 m depth ($1.07 \Omega \cdot \text{m}$). At G3, saline conditions are evident below 66.1 m ($0.115 \Omega \cdot \text{m}$), underlain by a brackish transition zone from $1.33\text{--}66.1 \text{ m}$ ($1.09 \Omega \cdot \text{m}$). G4 similarly shows deep saline signatures below 58.3 m ($0.12 \Omega \cdot \text{m}$), with a brackish interval above this depth ($1.72\text{--}8.21 \Omega \cdot \text{m}$).

The uppermost layers at all points exhibit elevated resistivity ($9\text{--}447 \Omega \cdot \text{m}$), attributable to unsaturated or freshwater-bearing sediments. Collectively, the four VES profiles demonstrate a consistent deep saline zone across the study area, reaffirming the inland penetration of seawater within the Kenjeran aquifer.

3.2. 2D Resistivity Profiles

The inversion results for Line 1 yielded an RMS error of 24.6%, as shown in Figure 2. Although this value is higher than ideal, the overall structure of the model remains consistent with the expected geological setting. The resistivity values along the profile span from approximately 0.1 to $32.8 \Omega \cdot \text{m}$, revealing clear contrasts between conductive and more resistive units. Very low resistivity values ($0.1\text{--}0.8 \Omega \cdot \text{m}$) appear in several discrete segments of the line, while intermediate values ($1\text{--}12 \Omega \cdot \text{m}$) and higher ranges ($>25 \Omega \cdot \text{m}$) form the surrounding units.

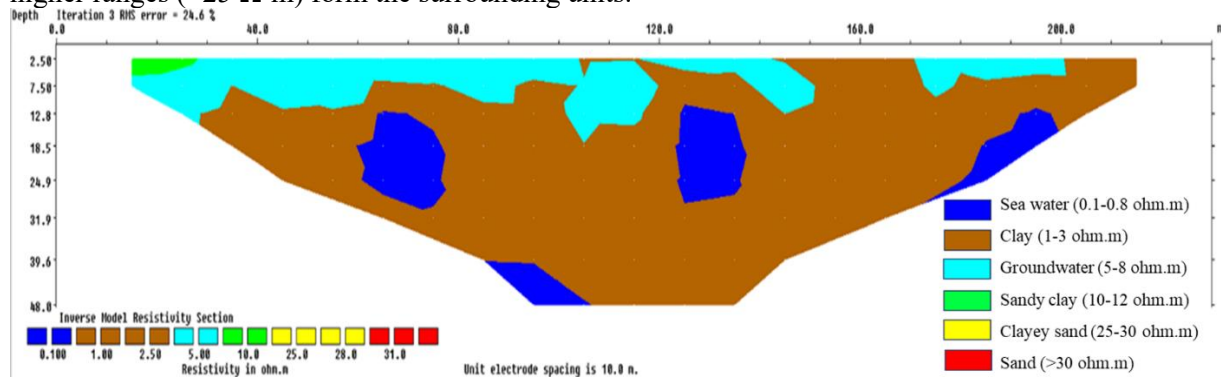


Figure 2. Interpreted 2D Resistivity Section of Line 1

Using the interpretation criteria established for this study, low resistivity zones ($0.1\text{--}0.8 \Omega \cdot \text{m}$) were initially attributed to seawater-affected sediments, whereas resistivities of $1\text{--}3 \Omega \cdot \text{m}$, $5\text{--}8 \Omega \cdot \text{m}$, $10\text{--}12 \Omega \cdot \text{m}$, and $25\text{--}30 \Omega \cdot \text{m}$ were associated with clay, freshwater-bearing material, sandy clay, and clayey sand, respectively. Clean sand corresponds to values above $\sim 30 \Omega \cdot \text{m}$. Along Line 1, four conductive zones—located at $60\text{--}75 \text{ m}$, $85\text{--}105 \text{ m}$, $125\text{--}135 \text{ m}$, and $175\text{--}200 \text{ m}$ —are interpreted as potential seawater intrusion features. These zones occur at depths of approximately $12\text{--}25 \text{ m}$ and $40\text{--}48 \text{ m}$, forming a pattern that suggests that seawater does not advance uniformly inland but follows pathways where permeability or hydraulic gradients favor deeper penetration.

The inversion of Line 2 yielded a slightly lower RMS error of 22.4% (Figure 3). The resistivity variations along this profile closely resemble those of Line 1, with low-resistivity features occurring at

30–50 m, ~65 m, 85–110 m, 130–160 m, and 160–235 m. These conductive bodies vary in thickness and depth, ranging between 7.5 m and 40 m below ground level. Compared to Line 1, Line 2 shows a more continuous pattern of conductive wedges, particularly toward the inland end of the profile, suggesting that seawater may be advancing through deeper channels or layers of relatively high permeability. The geometry observed here—narrow near-surface roots that widen at depth—is consistent with the typical shape of a saltwater intrusion wedge in unconfined coastal aquifers.

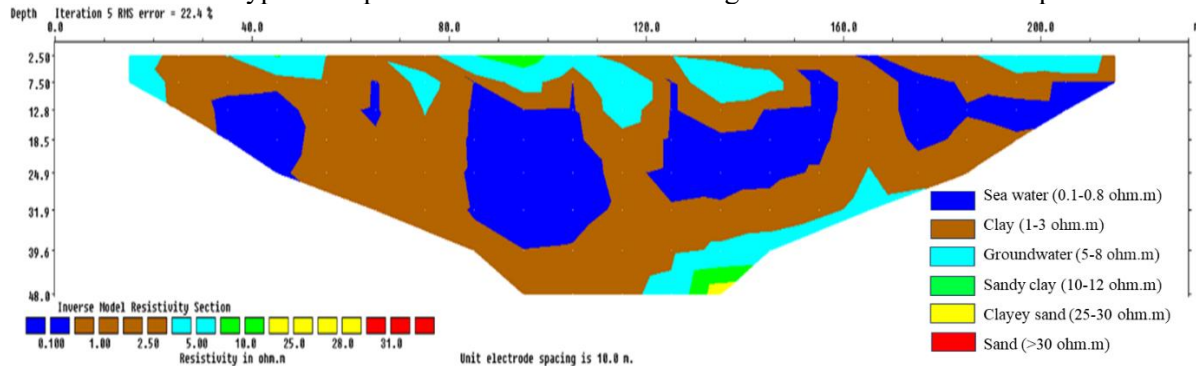


Figure 3. Interpreted 2D Resistivity Section of Line 2

A comparison of both profiles reveals that seawater intrusion is present along the entire surveyed section but manifests differently between the two lines. Line 1 exhibits more fragmented and isolated low-resistivity pockets, suggesting that intrusion there is controlled by localized variations in lithology or structural heterogeneity. In contrast, Line 2 displays a more continuous sequence of conductive wedges that extend farther inland and appear at relatively shallower depths (as shallow as 7.5 m). This pattern implies that the aquifer materials along Line 2 may possess higher permeability or better hydraulic connectivity, allowing saline water to propagate more effectively.

Despite these differences, both profiles share several common features: (1) the presence of deep conductive zones that become thicker toward the coast, and (2) clear resistive upper layers corresponding to freshwater-bearing sediments. Taken together, the two ERT lines indicate that seawater intrusion in the Kenjeran coastal aquifer is spatially heterogeneous, controlled by local lithological variations, and more pronounced along pathways where the subsurface is more permeable.

3.3. Comparation of 1D and 2D Resistivity Profiles

The 1D VES soundings (G1–G4) and the 2D ERT profiles (Line 1 and Line 2) provide complementary insights into the resistivity structure of the Kenjeran coastal aquifer. The VES data offer detailed vertical resolution at discrete locations and consistently show very low resistivity values ($<1 \Omega\cdot m$) at depths exceeding approximately 58–66 m, indicating the presence of deep saline groundwater. Above these intervals, the VES curves reveal intermediate resistivities (1–10 $\Omega\cdot m$) associated with brackish conditions, and higher resistivity values ($>30 \Omega\cdot m$) near the surface, which correspond to freshwater-bearing or unsaturated sediments. While the VES soundings effectively characterize depth-specific layering, their point-based nature limits the ability to visualize lateral continuity.

The 2D ERT profiles complement these findings by mapping resistivity variations continuously along the survey lines. Both Line 1 and Line 2 show multiple conductive zones (0.1–0.8 $\Omega\cdot m$) at depths of roughly 8–48 m, forming wedge-shaped geometries that thicken toward the coast. These wedges are interlayered with brackish and freshwater-bearing units and capture structural heterogeneity, such as subtle stratigraphic undulations and variable thicknesses of conductive layers, which cannot be resolved from the 1D data alone.

Because the G2 VES sounding lies near the central portion of ERT Line 2, these datasets allow for a direct comparison at a shared location. The G2 profile identifies a deep saline interval below approximately 64.9 m, underlain by a thick brackish zone extending to shallower depths. In Line 2, conductive anomalies between about 7.5 and 40 m depth coincide with the brackish-to-saline transition

observed at G2, even though the ERT system does not reach the full depth imaged by the VES. This spatial overlap indicates that the shallow and intermediate conductive bodies in Line 2 are connected to the deeper saline layer detected at G2, suggesting multiple pathways for seawater penetration influenced by local permeability variations.

We also compare the results with previous resistivity-based intrusion studies conducted in nearby coastal areas such as Sutorejo (East Surabaya). In their study, researchers used 2D resistivity along several transects in East Surabaya (including Sutorejo) and identified low-resistivity zones ($0.734\text{--}6.31\ \Omega\cdot\text{m}$) at shallow depth (0.6–3.5 m), interpreted as seawater intrusion [13]. This supports the plausibility of saline-water influence in coastal aquifers near urban Surabaya, albeit at much shallower depths than observed in Kenjeran. Moreover, earlier work using 2D IP/Resistivity in Surabaya Timur also revealed resistivities around $6.8\ \Omega\cdot\text{m}$ with low chargeability that likely correspond to saline groundwater [23]. Beyond Surabaya, similar resistivity-based seawater intrusion studies in other coastal settings, for example in a shallow aquifer along the western coast of Makassar. It demonstrated that conductive zones with resistivity as low as $0.2\text{--}1.8\ \Omega\cdot\text{m}$ at depths from a few meters to $> 30\ \text{m}$ correspond to saltwater-bearing layers [28]. Likewise, resistivity and hydrochemical analyses in the Tugu coastal area of Semarang identified low-resistivity intervals of approximately $3\text{--}6\ \Omega\cdot\text{m}$, corresponding to brackish silt-layer aquifers. The shallow unconfined aquifer is also dominated by silt with very low resistivity ($\sim 1.5\ \Omega\cdot\text{m}$), indicating the presence of saline or seawater-intruded groundwater [29]. Comparable findings were also reported in Desa Nusapati, Mempawah (West Kalimantan), where resistivity surveys detected values between approximately 0.15 and $1.88\ \Omega\cdot\text{m}$ within sandy aquifer layers influenced by saline water [30].

The similarity in resistivity ranges and intrusion signatures reinforces the interpretation that the conductive wedges and low-resistivity zones identified in Kenjeran are consistent with seawater intrusion phenomena documented in other coastal aquifers. This alignment indicates that the VES and ERT results from this study fall within a broader, well-established framework of coastal intrusion processes, thereby strengthening the validity of the interpretations made.

Taken together, the 1D and 2D datasets present a coherent and mutually reinforcing depiction of seawater intrusion in the study area. The VES soundings confirm the depth at which saline accumulation occurs, while the ERT profiles illustrate how these saline bodies extend laterally and vary in thickness and geometry. Their combined interpretation demonstrates that seawater intrusion in the Kenjeran aquifer is both vertically stratified and laterally heterogeneous, shaped by lithological variability and localized zones of enhanced hydraulic connectivity.

4. Conclusion

This study demonstrates the effectiveness of an integrated 1D Vertical Electrical Sounding (VES) and 2D Electrical Resistivity Tomography (ERT) approach for mapping seawater intrusion in the Kenjeran coastal aquifer, Surabaya. The 1D VES results delineate a consistent vertical stratification, identifying deep saline groundwater zones with very low resistivity ($< 1\ \Omega\cdot\text{m}$) at depths of approximately 58–66 m, overlain by brackish water layers ($1\text{--}10\ \Omega\cdot\text{m}$) and higher-resistivity near-surface units ($> 30\ \Omega\cdot\text{m}$). Complementarily, the 2D ERT sections provide detailed lateral and vertical imaging, revealing multiple wedge-shaped saline intrusion features ($0.1\text{--}0.8\ \Omega\cdot\text{m}$) extending from shallow to intermediate depths (8–48 m) and interbedded with brackish and freshwater zones, reflecting the influence of aquifer heterogeneity on intrusion pathways. The combined interpretation confirms that seawater intrusion in Kenjeran occurs through both lateral encroachment from the coastline and vertical penetration into deeper aquifer layers, and the observed resistivity ranges and intrusion geometries are consistent with findings from comparable resistivity-based studies in neighboring coastal regions. Overall, the integration of 1D and 2D resistivity methods provides a robust and reliable framework for characterizing the geometry and extent of seawater intrusion in urban coastal aquifers, offering essential geophysical evidence to support groundwater vulnerability assessment and sustainable coastal aquifer management.

Acknowledgements

The authors express gratitude for the contribution of funds through the financing scheme “Dana Penelitian Internal Universitas Pembangunan Nasional “Veteran” Jawa Timur Tahun Anggaran 2025 No. 166/UN.63/LPPM/2025.

References

- [1] P. M. Barlow and E. G. Reichard, “Saltwater intrusion in coastal regions of North America,” *Hydrogeol J*, vol. 18, no. 1, pp. 247–260, Feb. 2010, doi: [10.1007/s10040-009-0514-3](https://doi.org/10.1007/s10040-009-0514-3).
- [2] B. Winid and M. Maruta, “Assessment of Groundwater (Main Usable Aquifer) Vulnerability to Seawater Intrusion in the Polish Baltic Coastal Region,” *Water (Basel)*, vol. 17, no. 3, p. 336, Jan. 2025, doi: [10.3390/w17030336](https://doi.org/10.3390/w17030336).
- [3] S. Kalu, M. C. Ricker, J. Janson, D. Nordlund, and H. Li, “Destabilization of Soil Carbon After Saltwater Intrusion in Coastal Agricultural Soils,” *Environ Sci Technol*, vol. 59, no. 4, pp. 2107–2118, Feb. 2025, doi: [10.1021/acs.est.4c12966](https://doi.org/10.1021/acs.est.4c12966).
- [4] A. D. Werner *et al.*, “Seawater intrusion processes, investigation and management: Recent advances and future challenges,” *Adv Water Resour*, vol. 51, pp. 3–26, Jan. 2013, doi: [10.1016/j.advwatres.2012.03.004](https://doi.org/10.1016/j.advwatres.2012.03.004).
- [5] X. Cao, Q. Guo, and W. Liu, “Research on the Patterns of Seawater Intrusion in Coastal Aquifers Induced by Sea Level Rise Under the Influence of Multiple Factors,” *Water (Basel)*, vol. 16, no. 23, p. 3457, Dec. 2024, doi: [10.3390/w16233457](https://doi.org/10.3390/w16233457).
- [6] M. Debnath and N. Alamdari, “Impacts of Climate Change and Sea-Level Rise on Groundwater Levels and Saltwater Intrusion in Coastal Aquifers,” 2025. doi: [10.2139/ssrn.5085447](https://doi.org/10.2139/ssrn.5085447).
- [7] C. Dodd and G. M. Rishworth, “Coastal urban reliance on groundwater during drought cycles: Opportunities, threats and state of knowledge,” *Cambridge Prisms: Coastal Futures*, vol. 1, p. e11, Jan. 2023, doi: [10.1017/cft.2022.11](https://doi.org/10.1017/cft.2022.11).
- [8] S. Purnama, “Groundwater Vulnerability from Sea Water Intrusion in Coastal Area Cilacap, Indonesia,” *Indonesian Journal of Geography*, vol. 51, no. 2, p. 206, Aug. 2019, doi: [10.22146/ijg.18229](https://doi.org/10.22146/ijg.18229).
- [9] A. Abdillah, I. Widianingsih, R. A. Buchari, and H. Nurasa, “Adapting to climate change and multi-risk governance: toward sustainable adaptation and enhancing urban resilience—Indonesia,” *Discover Applied Sciences*, vol. 7, no. 1, p. 81, Jan. 2025, doi: [10.1007/s42452-025-06491-7](https://doi.org/10.1007/s42452-025-06491-7).
- [10] R. N. Indriastoni and I. Kustini, “INTRUSI AIR LAUT TERHADAP KUALITAS AIR TANAH DANGKAL DI KOTA SURABAYA,” *Rekayasa Teknik Sipil*, vol. 3, no. 4, pp. 228–232, 2014, Accessed: Jul. 31, 2025. [Online]. Available: <https://ejournal.unesa.ac.id/index.php/rekayasa-teknik-sipil/article/view/9519/9409>
- [11] F. Masitoh and B. A. Saifanto, “Pendugaan Kerentanan Airtanah Dangkal Terhadap Intrusi Airlaut Menggunakan Metode GALDIT di Kecamatan Sukolilo Kota Surabaya,” *Buletin Oseanografi Marina*, vol. 13, no. 2, pp. 153–165, Jun. 2024, doi: [10.14710/buloma.v13i2.53625](https://doi.org/10.14710/buloma.v13i2.53625).
- [12] A. Herdyansah and D. Rahmawati, “Dampak Intrusi Air Laut pada Kawasan Pesisir Surabaya Timur,” *Jurnal Teknik ITS*, vol. 6, no. 2, pp. 599–603, 2017.
- [13] R. R. Wardhana, D. D. Warnana, and A. Widodo, “Identifikasi Intrusi Air Laut Pada Air Tanah Menggunakan Metode Resistivitas 2D Studi Kasus Surabaya Timur,” *Jurnal Geosaintek*, vol. 3, no. 1, p. 17, Jan. 2017, doi: [10.12962/j25023659.v3i1.2946](https://doi.org/10.12962/j25023659.v3i1.2946).
- [14] D. A. Perdana, “Studi Intrusi Air Laut di Akuifer Dalam Menggunakan Peruntut Hidroisotop dan Analisis Hidrokimia. Studi Kasus: Kota Surabaya,” UNIVERSITAS GADJAH MADA, Yogyakarta, 2021. Accessed: Jul. 31, 2025. [Online]. Available: <https://etd.repository.ugm.ac.id/penelitian/detail/195862>

[15] M. M. Ramadhan and B. Hariyanto, “KAJIAN TENTANG AIR ASIN PADA AIRTANAH DANGKAL DI KECAMATAN KENJERAN KOTA SURABAYA,” *Swara Bhumi*, vol. 4, no. 3, pp. 24–33, 2017.

[16] W. M. Telford, L. P. Geldart, and R. E. Sheriff, *Applied Geophysics*. University of Cambridge, 1990. [Online]. Available: <https://books.google.co.id/books?id=oRP5fZYjhXMC&printsec=frontcover#v=onepage&q&f=false>

[17] A. Palacios *et al.*, “Time-lapse cross-hole electrical resistivity tomography (CHERT) for monitoring seawater intrusion dynamics in a Mediterranean aquifer,” *Hydrol Earth Syst Sci*, vol. 24, no. 4, pp. 2121–2139, Apr. 2020, doi: [10.5194/hess-24-2121-2020](https://doi.org/10.5194/hess-24-2121-2020).

[18] A. Pidlisecky, T. Moran, B. Hansen, and R. Knight, “Electrical Resistivity Imaging of Seawater Intrusion into the Monterey Bay Aquifer System,” *Groundwater*, vol. 54, no. 2, pp. 255–261, Mar. 2016, doi: [10.1111/gwat.12351](https://doi.org/10.1111/gwat.12351).

[19] A. Costall, B. Harris, and J. P. Pigois, “Electrical Resistivity Imaging and the Saline Water Interface in High-Quality Coastal Aquifers,” *Surv Geophys*, vol. 39, no. 4, pp. 753–816, Jul. 2018, doi: [10.1007/s10712-018-9468-0](https://doi.org/10.1007/s10712-018-9468-0).

[20] H. M. El-Sayed, M. I. A. Ibrahim, A.-S. Abou Shagar, and A. R. Elgendi, “Geophysical and hydrochemical analysis of saltwater intrusion in El-Omayed, Egypt: Implications for sustainable groundwater management,” *Egypt J Aquat Res*, vol. 49, no. 4, pp. 478–489, Dec. 2023, doi: [10.1016/j.ejar.2023.11.005](https://doi.org/10.1016/j.ejar.2023.11.005).

[21] B. M. Niculescu and G. Andrei, “Application of electrical resistivity tomography for imaging seawater intrusion in a coastal aquifer,” *Acta Geophysica*, vol. 69, no. 2, pp. 613–630, Apr. 2021, doi: [10.1007/s11600-020-00529-7](https://doi.org/10.1007/s11600-020-00529-7).

[22] M. Hasan, Y. Shang, G. Akhter, and W. Jin, “Application of VES and ERT for delineation of fresh-saline interface in alluvial aquifers of Lower Bari Doab, Pakistan,” *J Appl Geophy*, vol. 164, pp. 200–213, May 2019, doi: [10.1016/j.jappgeo.2019.03.013](https://doi.org/10.1016/j.jappgeo.2019.03.013).

[23] B. Aryaseta, D. D. Warnana, and A. Widodo, “Identifikasi Intrusi Air Laut pada Air Tanah Menggunakan Induced Polarization Studi Kasus Daerah Surabaya Timur,” *Jurnal Geosaintek*, vol. 2, no. 3, 2016.

[24] B. M. Niculescu and G. Andrei, “Using Vertical Electrical Soundings to characterize seawater intrusions in the southern area of Romanian Black Sea coastline,” *Acta Geophysica*, vol. 67, no. 6, pp. 1845–1863, Dec. 2019, doi: [10.1007/s11600-019-00341-y](https://doi.org/10.1007/s11600-019-00341-y).

[25] D. Tarallo, I. Alberico, G. Cavuoto, N. Pelosi, M. Punzo, and V. Di Fiore, “Geophysical assessment of seawater intrusion: the Volturno Coastal Plain case study,” *Appl Water Sci*, vol. 13, no. 12, p. 234, Dec. 2023, doi: [10.1007/s13201-023-02033-x](https://doi.org/10.1007/s13201-023-02033-x).

[26] R. Martorana, P. Capizzi, A. D’Alessandro, and D. Luzio, “Comparison of different sets of array configurations for multichannel 2D ERT acquisition,” *J Appl Geophy*, vol. 137, pp. 34–48, Feb. 2017, doi: [10.1016/j.jappgeo.2016.12.012](https://doi.org/10.1016/j.jappgeo.2016.12.012).

[27] M. H. Loke, J. E. Chambers, D. F. Rucker, O. Kuras, and P. B. Wilkinson, “Recent developments in the direct-current geoelectrical imaging method,” *J Appl Geophy*, vol. 95, pp. 135–156, Aug. 2013, doi: [10.1016/j.jappgeo.2013.02.017](https://doi.org/10.1016/j.jappgeo.2013.02.017).

[28] L. M. Mas’ud, A. Azikin, H. Umar, and H. Zubair, “Delineation of Seawater Intrusion, Using Geo-Electric Resistivity Method, in Shallow Aquifer in Western Part of Makassar, South Sulawesi, Indonesia,” *The Iraqi Geological Journal*, pp. 109–123, Oct. 2024, doi: [10.46717/igj.57.2D.9ms-2024-10-19](https://doi.org/10.46717/igj.57.2D.9ms-2024-10-19).

[29] S. Widada, B. Rochaddi, C. A. Suryono, and I. Irwani, “Intrusi Air Laut di Pesisir Tugu Kota Semarang Berdasarkan Resistiviti dan Hidrokimia,” *Jurnal Kelautan Tropis*, vol. 21, no. 2, p. 75, Dec. 2018, doi: [10.14710/jkt.v21i2.3610](https://doi.org/10.14710/jkt.v21i2.3610).

[30] Muhardi, Faurizal, and Widodo, “Analisis Pengaruh Intrusi Air Laut terhadap Keberadaan Air Tanah di Desa Nusapati, Kabupaten Mempawah Menggunakan Metode Geolistrik Resistivitas,” *Indonesian Journal of Applied Physics*, vol. 10, no. 2, p. 89, Oct. 2020.